sciendo

DOI: 10.2478/ata-2022-0022

Acta Technologica Agriculturae 3
Nitra, Slovaca Universitas Agriculturae Nitriae, 2022, pp. 144–149

COMPRESSIVE LOADING OF APPLE CULTIVAR GOLDEN DELICIOUS

Ľubomír KUBÍK*, Viera KAŽIMÍROVÁ, Monika BOŽIKOVÁ

Slovak University of Agriculture in Nitra, Slovakia

The study dealt with the experimental and numerical assessment of the apple cultivar Golden Delicious (*Malus domestica* L.) at compressive loading in lateral direction. The development of fruit hemisphere behaviour was examined between two parallel plates. Apple samples were subjected to tests at different strain rates. The experiments were conducted at eleven velocities from 10 to 350 mm·min^{-1} for the purposes of achieving different strain rates. Compression tests of the fruits at different strain rates corresponded to the quasi-state loading. Impacts of loading rate and strain rate on force and stress at compression were studied. The material exhibited nonlinear behaviour of dependency of stresses on strains, but linear viscoelastic behaviour of dependency of stresses on strain rate. The application possibilities of Kelvin-Voight viscoelastic model were evaluated. Forces, strains, stresses and the apparent moduli of elasticity were evaluated for the detection of fruit damage at different strain rates.

Keywords: fruit behaviour; compression; strain rate; loading rate

The instrumental firmness of apples changes significantly during shelf life, whereas the sensory attributes do not change significantly for each cultivar or attribute, confirming the advantages of instrumental firmness measurements compared over the sensory evaluation (Zdunek et al., 2011). The compression test of fruits at different strain rates corresponds to quasi-state loading (Severa, 2008). Strain rate has an effect on the material stress. The eating qualities of the apple flesh are dependent on fruit textures (Khan and Vicent, 1993). The key quality parameter of the flesh is firmness. The fruit ripeness is directly related to fruit (Farris et al., 2008). Apples and potatoes are sensitive to impacts of pressure, as it causes cracking and crushing in tissues. The study of turgor pressure and the compressive stiffness of apple and potato tissues play vital roles in comprehension of their fracture strength against external and internal pressures (Singh et al., 2014). Farris et al. (2008) investigated the apples of varieties Golden Delicious and Pink Lady. They conducted a bending-snapping test and a modified compression-relaxation test. Moreover, the differentiation between osmo-air-dried apple rings as a function of variety and drying temperature (from 70 °C to 90 °C) were performed. Costa et al. (2011) presented the simultaneous measurements of mechanical and acoustic response of the apple tissue to compression. In their research, the apple cultivars (86 varieties) were examined after two months postharvest storage and 16 acoustic and mechanical parameters were used for testing. Costa (2016) investigated the peel contribution to common apple firmness using texture analyser, by which a collection of 65 accessions after two months of cold storage was examined. The mechanical force-displacement quantities were determined, and a set of analytical parameters was derived on the basis of those quantities. Blahovec (1999) studied stored apples and raw cherries, which were measured by the quasi-static compression of simple fruits between two plates, and investigated their defect resistance coefficient and destruction sensitivity, reaching a conclusion that increasing of compression influenced the changes in resistance and sensitivity. Rao and Brown (2011) measured the modulus and failure strength of skins of apple varieties stored under controlled atmosphere. Puncture force values of McIntosh, Red Delicious and Empire were lower in contrast to Crimson Gala and Honey Crisp. Skin peak force of the Honey Crisp apples was least among all the studied apples. Fazel et al. (2020) observed that the stress acting on the fruit surface during harvest, transport and storage leads to tissue bruising and eventually results in fruit failure. For this reason, prediction of bruise volume and mechanical properties caused by impacts and compression play an essential role in each of the aforementioned operations.

The study of apple hemispheres in the compression between two parallel plates was conducted according to the recommendations of the ASAE S368.4 (2008). The effects of loading and strain rates on force and stress at compression were studied. Furthermore, the application possibilities of linear viscoelastic model were evaluated. Forces, strains, stresses and the apparent moduli of elasticity were determined to describe the fruit deformation during storage.

Material and methods

The paper presented examines subjecting of the apple fruits of cultivar Golden Delicious (*Malus domestica* L.) to compression loading. Apple samples came from village Tekovská Breznica (coordinates 48° 22′ 59″ N and 18° 37′ 1″ E), region Žarnovica in Slovakia. Apple trees were planted in

Contact address: Ľubomír Kubík, Slovak University of Agriculture in Nitra, Faculty of Engineering, Tr. Andreja Hlinku 2, 949 76 Nitra, Slovakia, e-mail: Lubomir.Kubik@uniag.sk

the espalier-style growing as the full-size trees. The orchard was situated on the mild slope oriented to the north-west in Štiavnické vrchy in the altitude of 197 m. The trees were cultivated on the cambisol soil type. The trees were protected against the wind and the air draught by plastic lattices. The average region maximum day temperature is 19 °C. At the end of September 2020 (harvest), the maximum day temperatures recorded ranges from 13 to 20 °C. Apple samples were harvested at the end of September 2020. The fruits were stored during one day after harvesting in the refrigerator at 4 °C temperature and 40–60% air humidity. Subsequently, the fruits were immediately subjected to the tests presented.

Six fruit samples were collected and used for testing. Each fruit was cut into two hemispheres. Twelve samples were used for each loading. Eleven samples were suitable for elaboration. Loading was realized as the hemisphere compression between two parallel plates (Severa, 2008; Nedomová et al., 2017). For the purposes of sample testing, statical compressive loading in lateral direction was employed. Compression tests were performed using a testing machine Andilog Stentor 1000 (Andilog Technologies, Vitrolles, France). The experiments were conducted at eleven velocities from 10 to 350 mm·min^{-1} with the aim to achieve different strain rates (Severa, 2008).

Strain rate $\frac{d\varepsilon}{dt}$ is defined as deformation change per time:

$$\frac{d\varepsilon}{dt}=\frac{d}{dt}\left(\frac{\Delta l}{l_0}\right)=\frac{d}{dt}\left(\frac{l-l_0}{l_0}\right)=\frac{1}{l_0}\frac{dl}{dt}=\frac{v}{l_0} \quad (1)$$

where: ε – deformation; Δl – contraction; l_0 – initial length; l – length after contraction; v – speed; t – time; $\frac{d}{dt}$ – time derivation

Force F (N) and compression D_c (m) were measured via the acquisition software RSIC ver. 4.06. The dependency loading curves of force on deformation and dependency curves of stress on strain were plotted. Furthermore, the influences of the loading speed of testing machine on force and the effect of strain rate on stress were studied and assessed. Loading rate represents the speed at which forces are applied to the material. The apparent moduli of elasticity of the apple hemispheres compressed between two parallel plates (Fig. 1) were determined on the basis of Hertz theory (ASAE S368.4, 2008):

$$E_a=\frac{0.338\,K^{\frac{3}{2}}F(1-\mu^2)}{D_d^{\frac{3}{2}}}\left[\left(\frac{1}{R_U}+\frac{1}{R'_U}\right)^{\frac{1}{2}}\right] \quad (2)$$

where: E_a – elasticity modulus; D_c – compression; μ – Poisson's ratio; F – force; R_U, R'_U – minimum and maximum radii of curvature of the sample convex surface; K – constant determined on the basis of contact angle

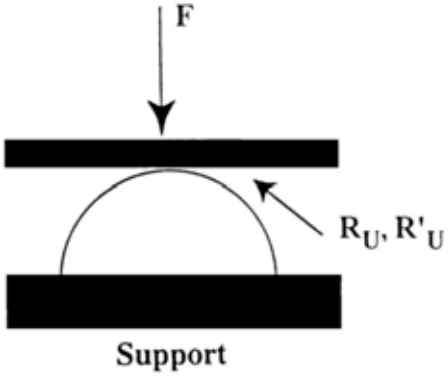


Fig. 1 Compression of the apple hemisphere between two parallel plates

Results and discussion

The compression procedure of fruit hemisphere between two parallel plates is presented in Fig. 2. The sample parameters, loading speeds and strain rates are outlined in Table 1. The force-deformation dependences are provided in Fig. 3, indicating the evident effect of loading rate on force during the hemisphere compression between two parallel plates. The uncertainties of force and deformation measurements were ±0.05 N and ±0.01 mm, respectively. The values are parameters of the testing machine Andilog Stentor 1000. The force uncertainties were from 0.01% at 500 N to 50% at 0.1 N deformation. The deformation uncertainties were from 10% at 0.1 mm to 0.01% at 7 mm. The regression equations are shown in Table 2, comparing the quadratic, cubic and power regression models and indicating the power function to be the best model. The curves are shifted by the effect of applied speed at loading and loading rate.



Fig. 2 Hemisphere compression between two parallel plates

Table 1 Parameters of the hemisphere samples

No.	R_U (mm)	R'_U (mm)	S (mm^2)	v (mm·min^{-1})	v (mm·s^{-1})	Strain rate (s^{-1})
1	33.48	35.60	3741.97	10	0.1667	0.0047
2	30.78	29.20	2821.70	20	0.3333	0.0114
3	33.25	35.35	3690.72	30	0.5000	0.0141
4	30.90	33.80	3279.48	50	0.8333	0.0247
5	31.53	32.60	3227.03	80	1.3333	0.0409
6	28.03	31.90	2807.15	100	1.6667	0.0522
7	28.85	32.15	2912.44	150	2.5000	0.0778
8	33.65	30.50	3222.66	200	3.3333	0.1093
9	33.15	31.90	3320.50	250	4.1667	0.1306
10	31.93	31.80	3187.78	300	5.0000	0.1572
11	34.60	36.90	4008.96	350	5.8333	0.1581

n – number of samples; R_U, R'_U – polar and the radial radii of curvature of sample surface; S – elliptical area of the sample section; v – speed/loading rate

Table 2 Regression equations of the force-deformation curves (Fig. 3)

v (mm·min^{-1})	Strain rate (s^{-1})	Regression equations	Coefficient of determination
10	0.005	$y = 3.375x^{2.461}$	$R^2 = 0.9741$
20	0.011	$y = 15.733x^{1.696}$	$R^2 = 0.9904$
30	0.014	$y = 1.829x^{2.888}$	$R^2 = 0.9756$
50	0.025	$y = 0.979x^{3.491}$	$R^2 = 0.9047$
80	0.041	$y = 11.34x^{1.855}$	$R^2 = 0.9979$
100	0.052	$y = 16.063x^{1.665}$	$R^2 = 0.9927$
150	0.078	$y = 1.006x^{2.96}$	$R^2 = 0.9442$
200	0.109	$y = 3.082x^{2.202}$	$R^2 = 0.9695$
250	0.131	$y = 8.014x^{1.857}$	$R^2 = 0.9981$
300	0.157	$y = 1.003x^{3.114}$	$R^2 = 0.8951$
350	0.158	$y = 0.607x^{3.203}$	$R^2 = 0.8937$

Table 3 Regression equations of the stress-strain curves (Fig. 4)

v (mm·min^{-1})	Strain rate (s^{-1})	Regression equations	Coefficient of determination
10	0.005	$y = 4802.4x^{2.361}$	$R^2 = 0.9877$
20	0.011	$y = 2403.3x^{1.844}$	$R^2 = 0.9990$
30	0.014	$y = 5066.2x^{2.434}$	$R^2 = 0.9904$
50	0.025	$y = 3858.0x^{2.306}$	$R^2 = 0.9579$
80	0.041	$y = 2542.9x^{1.914}$	$R^2 = 0.9935$
100	0.052	$y = 1855.7x^{1.683}$	$R^2 = 0.9916$
150	0.078	$y = 3307.7x^{2.453}$	$R^2 = 0.9469$
200	0.109	$y = 10593x^{2.701}$	$R^2 = 0.8762$
250	0.131	$y = 1889.7x^{2.011}$	$R^2 = 0.9853$
300	0.157	$y = 2012.6x^{2.158}$	$R^2 = 0.9233$
350	0.158	$y = 1359.8x^{1.976}$	$R^2 = 0.9724$

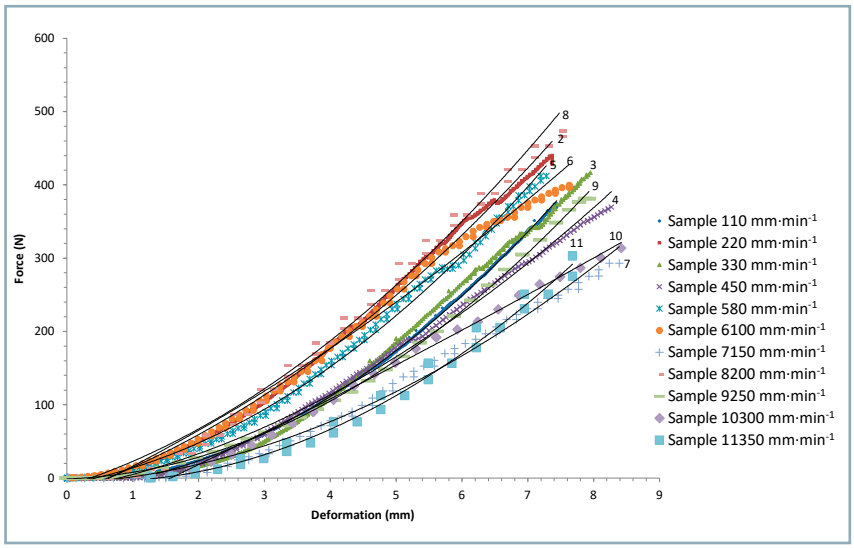


Fig. 3 Effects of loading rate on force during the hemisphere compression between two parallel plates at different loading rates

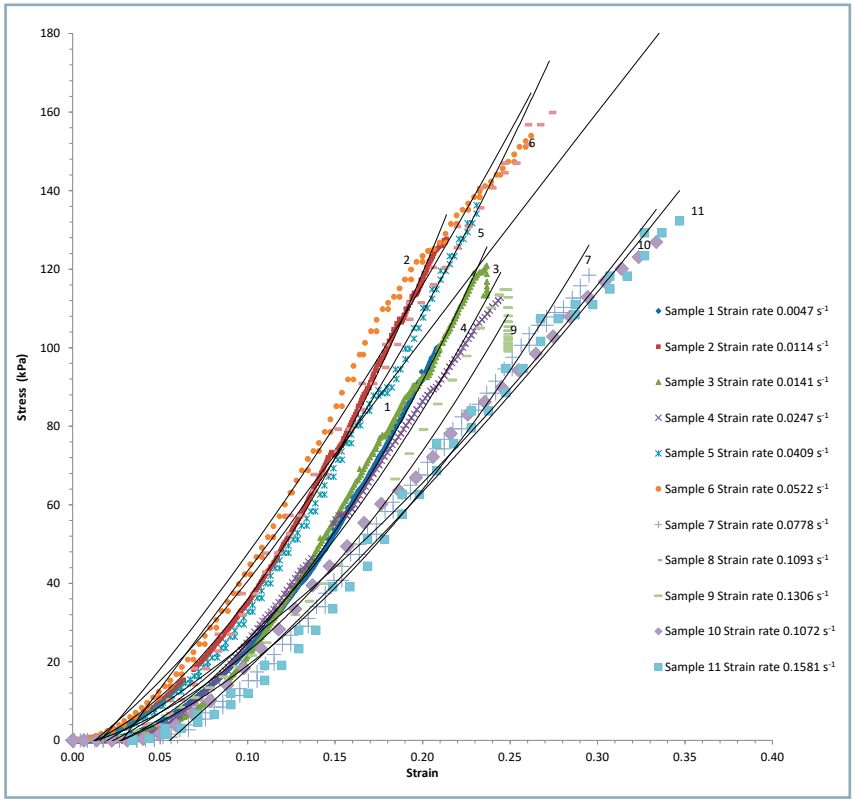


Fig. 4 Effects of loading rate on stress during the compression of hemispheres between two parallel plates at different strain rates

Table 4 Constants of Kelvin model (Fig. 5)

Strain	η (kPa·s)	σ_0 (kPa)
0.1	40.508	31.66
0.2	220.07	105.34
0.3	587.28	218.98

Furthermore, data were also converted into stress-strain dependences (Fig. 4). Jafarian et al. (2021) studied the effects of impact loads on Golden Delicious apples, which were determined by measuring bruise volume and bruise susceptibility. The measuremenaat uncertainties of stress and strain were performed using the method of indirect measurements by the derivation of definition equations of stress and strain and with application of the uncertainties of deformation and force. The measurement uncertainties of stresses and strains were ±0.116 kPa and ±0.002, respectively. The stress uncertainties ranged from 0.08% at 150 KPa to 116% at 0.1 kPa. The strain uncertainties ranged from 20% at a value of 0.01 to 0.67% at a value of 0.3. The regression equations are provided in Table 3, comparing the quadratic, cubic and power regression models. The power function showed the best results. Moreover, the loading rate effect on strain during the hemisphere compression between two parallel plates is evident. The curves are shifted due to the effect of applied speed at loading and loading rate.

The strain rate influence on stress is shown in Fig. 5. The dependences were plotted for the strain values of 0.1, 0.2 and 0.3, respectively.

As it is possible to observe in Fig. 5, material exhibited a typical linear viscoelastic behaviour (Severa, 2008). The Kelvin-Voigt model of viscoelasticity is described as follows:

$$\sigma = E\varepsilon + \eta\dot{\varepsilon} = \sigma_0 + \eta\dot{\varepsilon} = a + b\dot{\varepsilon} \qquad (3)$$

where: σ – stress (Pa); σ_0 – initial stress (Pa); E – modulus of elasticity (Pa); ε – strain; $\dot{\varepsilon}$ – strain rate (s^{-1}); η – dynamic viscosity (Pa·s); a, b – regression constants

The regression equations in Fig. 5 were determined and their forms correspond with the Kelvin model (Eq. 3) of stresses at the strain values of 0.1, 0.2 and 0.3 (Table 4).

Apparent moduli of elasticity were determined on the basis of Eq. 2. Poisson's ratio μ was assumed to be 0.22 (ASAE S368.4, 2008). K was the constant determined based on contact angle, K = 1.349 (ASAE S368.4, 2008). The apparent moduli of elasticity

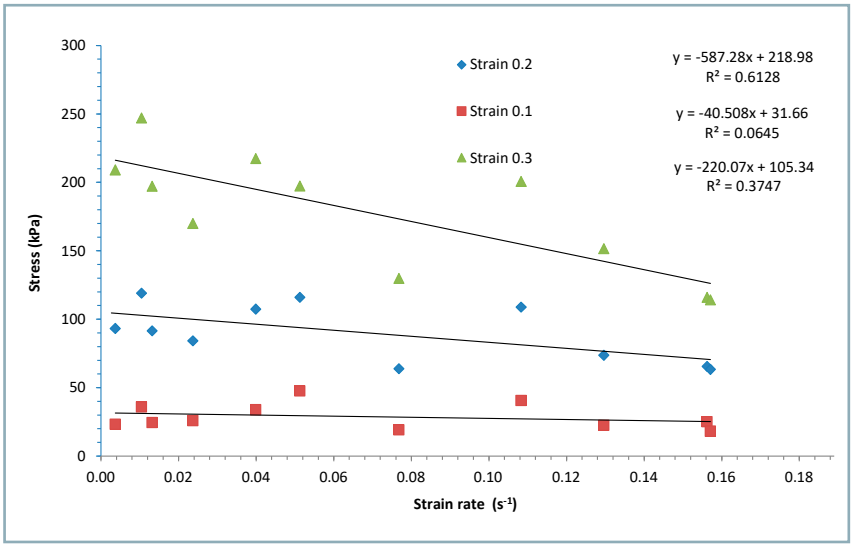


Fig. 5 Strain rate effect on stress at the strain values of 0.1, 0.2 and 0.3 during hemisphere compression between two parallel plates

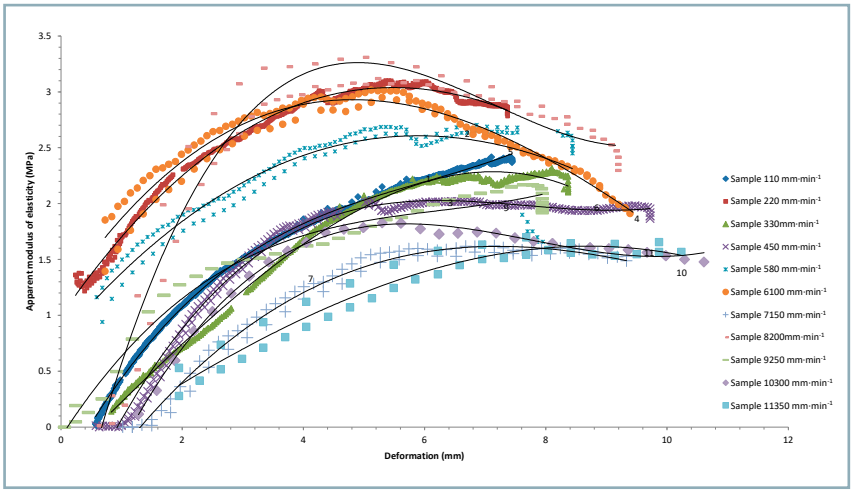


Fig. 6 Dependences of the moduli of elasticity on deformation during hemisphere compression between two parallel plates

depended on the value of deformation D_c (mm). Dependencies are presented in Fig. 6. Regression equations are shown in Table 5. Quadratic, cubic and power regression models were compared, the best model proved to be the cubic function. Considering the level of deformation 1–9 mm arising due to the compression between two parallel plates, the experimental data of the apparent moduli of elasticity reached the values of 0.5–3 MPa. The measurement uncertainties of apparent moduli of elasticity at a deformation value of 7 mm were on the level 26.25 KPa and on the level 76.83 KPa at a compression value of 1 mm, i.e., the apparent modulus of elasticity uncertainties ranged from 5.25% at 1 mm deformation to 2.56% at 7 mm deformation.

In their research of the apple Starkrimson peel, Wang et al. (2015) observed the maximum values of tensile strength, elastic modulus, fracture strain, tear strength, and puncture strength of 2.56 MPa, 24.00 MPa, 19.92%, 0.391 kN·m^{-1}, and 0.289 N·mm^{-2}, respectively. Arrieta-Baez et al. (2020) came to conclusion that the results obtained in their work may facilitate a better comprehension of mechanical properties of the apple fruit skin, which are essentially associated with the specific aliphatic composition of cutins, and further aid in investigation of microcrack formation. Vasighi-Shojae et al. (2020) studied the quality factors of Golden Delicious. The authors measured

Table 5 Regression equations of the moduli of elasticity-deformation curves (Fig. 6)

v (mm·min^{-1})	Strain rate (s^{-1})	Regression equations	Coefficient of determination
10	0.005	$y = 0.0079x^3 - 0.1416x^2 + 1.004x - 0.4351$	$R^2 = 0.9988$
20	0.011	$y = 0.0014x^3 - 0.0837x^2 + 0.7885x + 0.9946$	$R^2 = 0.9937$
30	0.014	$y = -0.0038x^3 + 0.0029x^2 + 0.5361x - 0.3116$	$R^2 = 0.9951$
50	0.025	$y = 0.0075x^3 - 0.1732x^2 + 1.2797x - 1.0464$	$R^2 = 0.9889$
80	0.041	$y = 0.0008x^3 - 0.0611x^2 + 0.6404x + 0.798$	$R^2 = 0.8232$
100	0.052	$y = 0.0031x^3 - 0.1061x^2 + 0.8054x + 1.1648$	$R^2 = 0.9459$
150	0.078	$y = 0.0023x^3 - 0.0827x^2 + 0.8337x - 0.9552$	$R^2 = 0.9874$
200	0.109	$y = 0.0167x^3 - 0.3577x^2 + 2.3011x - 1.3922$	$R^2 = 0.9529$
250	0.131	$y = 0.0052x^3 - 0.1091x^2 + 0.8019x - 0.0697$	$R^2 = 0.9619$
300	0.157	$y = 0.0082x^3 - 0.1918x^2 + 1.384x - 1.3626$	$R^2 = 0.9951$
350	0.158	$y = -0.0009x^3 - 0.0089x^2 + 0.3711x - 0.3093$	$R^2 = 0.9535$

apples utilizing ultrasound method and predicted the mechanical properties, including firmness, modulus of elasticity and stiffness of apples. The modulus of elasticity measured was equal to 0.0087 MPa and the predicted was equal to 0.0117 MPa. Shirvani et al. (2014) evaluated three theories (Hooke, Hertz and Boussinesq) in terms of the apparent modulus of elasticity of specific apple varieties, i.e., Golden Delicious, Red Delicious and Granny Smith. Hertz's theory was recommended as the most appropriate method due to easiness of application on a cylindrical sample of apple and close compliance with reality. Based on the results of their study, Golden Delicious and Granny Smith varieties showed the lowest and the highest moduli of elasticity – 2.211 MPa and 3.431 MPa, respectively. Zhu et al. (2022) applied the different compression forces (0, 40, 80, 160, 320, 640 N) to the apple equator. The experiments showed that the apples do not get damaged if compressive force is lower than 40 N. On the other hand, the weight loss of harvested apples under compressive forces of 80, 160, 320, and 640 N significantly increased, and fruits were damaged.

Conclusion

The measurements confirmed the loading rate effect on compressive force or compressive stress during the compression of fruit hemispheres between two parallel plates.

Damage to the fruit is descriptible by the compression method. Forces and stresses decreased with increased strain rate.

Variations in force were caused by different cross sections of hemispheres. The strain rate effect on compressive stress during the compression of fruit hemispheres between two parallel plates showed linear viscoelastic character described by Kelvin model.

The apparent moduli of elasticity obtained on the basis of the contact Hertz theory of solid body for the lateral loading of the hemispheres between two parallel plates were consistent. The apparent modulus of elasticity values depended on deformation; the moduli decreased with increasing strain rate.

Acknowledgements

This publication was supported by the Operational Programme Integrated Infrastructure within the project: Demand-driven research for sustainable and innovative food, Drive4SIFood 313011V336, co-financed by the European Regional Development Fund.

References

ASAE S368.4: 2008. Compression Test of Food Materials of Convex Shape. American Society of Agricultural Engineers, 2950, Niles Road, ST. Joseph, MI, USA.

ARRIETA-BAEZ, D. – PEREA FLORES, M. D. – MÉNDEZ-MÉNDEZ, J. V. – MENDOZA LEÓN, H. F. – GÓMEZ-PATIÑO, M. B. 2020. Structural studies of the cutin from two apple varieties: Golden Delicious and Red Delicious (*Malus domestica*). In Molecules, vol. 25, no. 24, article no. 5955.

BLAHOVEC, J. 1999. Bruise resistance coefficient and bruise sensitivity of apples and cherries. In International Agrophysics, vol. 13, no. 3, pp. 315–321.

COSTA, F. – CAPPELLIN, L. – LONGHI, S. – GUERRA, W. – MAGNAGO, P. – PORRO, D. – SOUKOULIS, C. – SALVI, S. – VELASCO, R. – BIASIOLI, F. – GASPERI, F. 2011. Assessment of apple (*Malus* × *domestica* Borkh.) fruit texture by a combined acoustic-mechanical profiling strategy. In Postharvest Biology and Technology, vol. 61, no. 1, pp. 21–28.

COSTA, F. 2016. Mechanical investigation to assess the peel contribution in apple fruit. In Postharvest Biology and Technology, vol. 111, pp. 41–47.

FARRIS, S. – GOBBI, S. – TORREGGIANI, D. – PIERGIOVANNI, L. 2008. Assessment of two different rapid compression tests for the evaluation of texture differences in osmo-air-dried apple rings. In Journal of Food Engineering, vol. 88, no. 4, pp. 484–491.

JAFARIAN, M. – EMAMI, H. – BARADARAN MOTIE, J. 2021. Effect of $Ca(NO_3)$ coating on chemical and mechanical properties and bruise susceptibility of Golden Delicious and Red Delicious apples during storage. In Acta Alimentaria, vol. 50, no. 3, pp. 404– 416.

KHAN, A. A. – VINCENT, J. V. F. 1993. Anisotropy in the fracture properties of apple flesh as investigated by crack-opening tests. In Journal of Material Sciences, vol. 28, pp. 45–51.

FAZEL, F. – GOLMOHAMMADI, A. – SHAHGHOLI, G. –AHMADI, E. 2020. Predictions of the apple bruise volume on the basis of impact energy or maximum contact force using adaptive neuro-fuzzy inference system (ANFIS). In Acta Technologica Agriculturae, vol. 23, no. 3, pp. 118–125.

NEDOMOVÁ, Š. – KUMBÁR, V. – PYTEL R. – BUCHAR, J. 2017. Mechanical properties of sugar beet root during storage. In International Agrophysics, vol. 31, no. 4, pp. 507–513.

RAO, M. A. – BROWN, S. K. 2011. Rheological characteristics of apple skin and apple firmness. In International Journal of Food Properties, vol. 14, no. 6, pp. 1297–1304.

SEVERA, L. 2008. Behaviour of the peach under underwater shock wave loading. In Acta Universitatis Agriculturae et Silviculturae Mendelianae Brunensis, vol. 56, no. 4, pp. 151–159.

SHIRVANI, M. – GHANBARIAN, D. – GHASEMI-VARNAMKHASTI, M. 2014. Measurement and evaluation of the apparent modulus of elasticity of apple based on Hooke's, Hertz's and Boussinesq's theories. In Measurement, vol. 54, pp. 133–139.

SINGH, F. – KATIYARA, V. K. – SINGH, B. P. 2014. Analytical study of turgor pressure in apple and potato tissues. In Postharvest Biology and Technology, vol. 89, pp. 44–48.

VASIGHI-SHOJAE, H. – GHOLAMI-PARASHKOUHI, M. – MOHAMMADZAMANI, D. – SOHEILI, A. 2020. Predicting mechanical properties of Golden Delicious apple using ultrasound technique and artificial neural network. In Food Analytical Methods, vol. 13, no. 3, pp. 699–705.

WANG, J. – CUI, Q. – LI, H. – LIU, Y. 2015. Experimental research on mechanical properties of apple peels. In Journal of Engineering and Technological Sciences, vol. 47, no. 6, pp. 688–705.

ZDUNEK, A. – CYBULSKA, J. – KONOPACKA, D. – RUTKOWSKI, K. 2011. Inter-laboratory analysis of firmness and sensory texture of stored apples. In International Agrophysics, vol. 25, no. 1, pp. 67–75.

ZHU, J. – ZHU, D. – WANG, L. – XUE, K. – LIAO, J. – ZHANG, S. 2022. Effects of compression damage on mechanical behavior and quality attributes of apple fruit. In Food Science and Technology Research, vol. 28, no. 1, pp. 53–65.